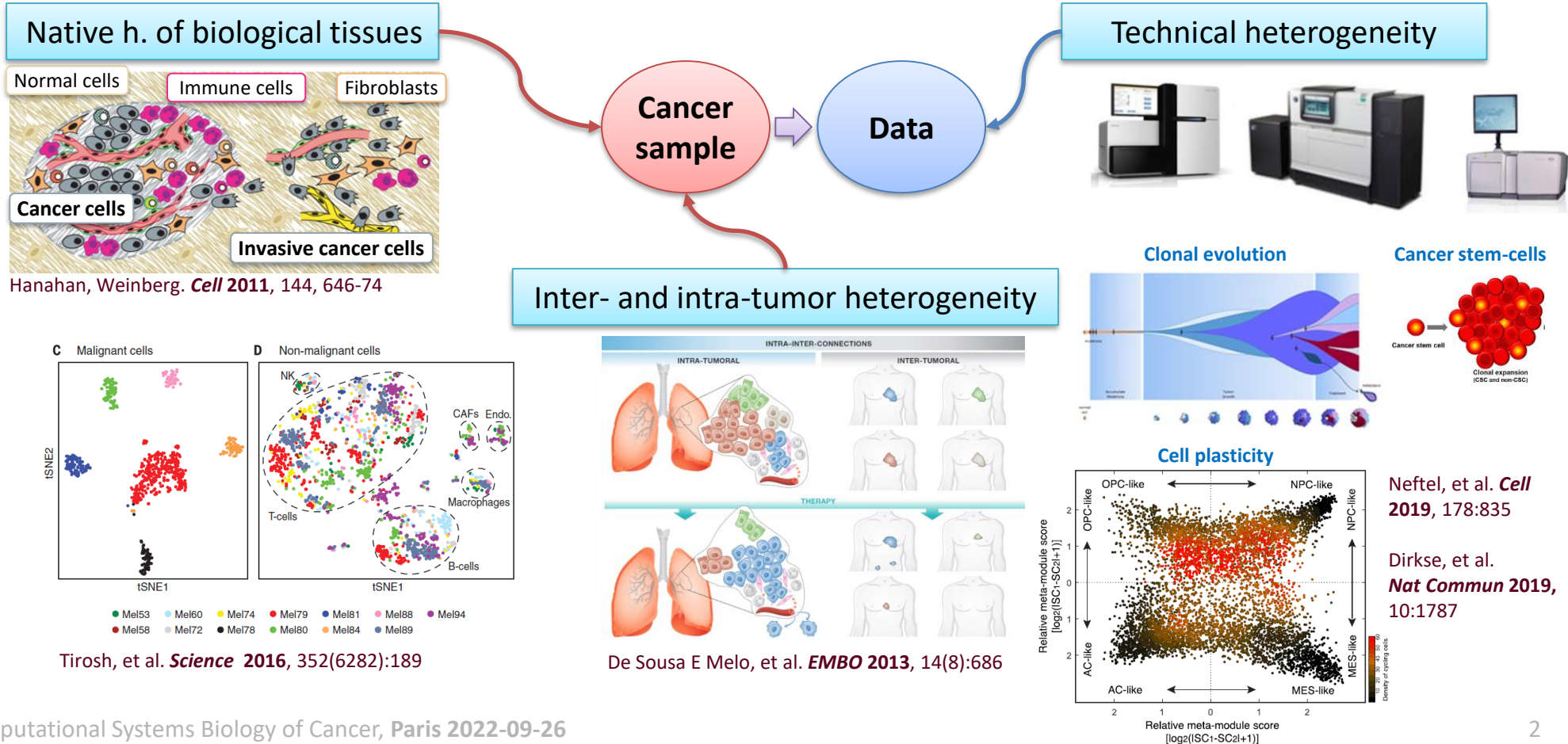


Combination of Multi-modal Data for Improved Patient Characterization

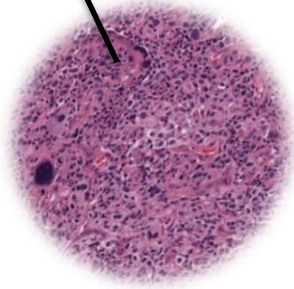
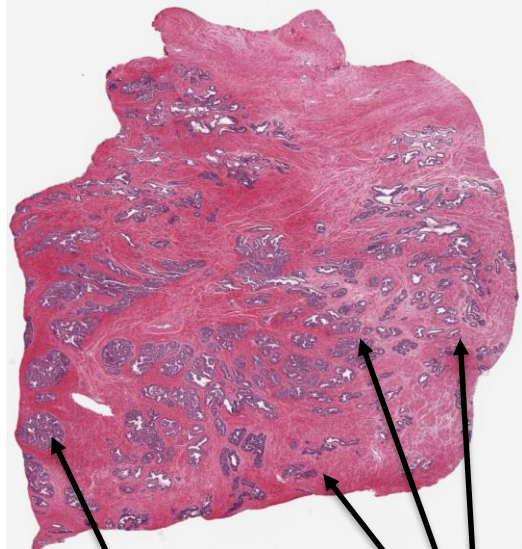
Petr Nazarov

5th course on Computational Systems Biology of Cancer
September 26-30, 2022 – Institut Curie, Paris, France

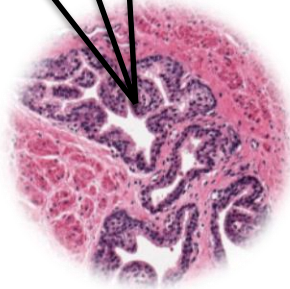
Levels of Heterogeneity in Samples of Cancer Patients



Hematoxylin and Eosin (H&E) stain



Tumor: 1%



Normal: 99%

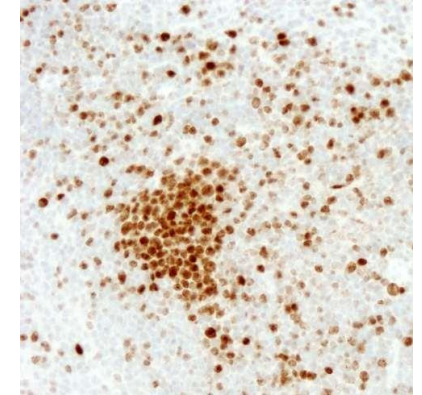
Features of histopathology

- Gold standard!
- Cheap (H&E or 2-3 antibodies in IHC)
- Captures native heterogeneity of tissues
- Shows inter/intra tumor heterogeneity
- Often allows precise diagnostics

Issues in histopathological image analysis:

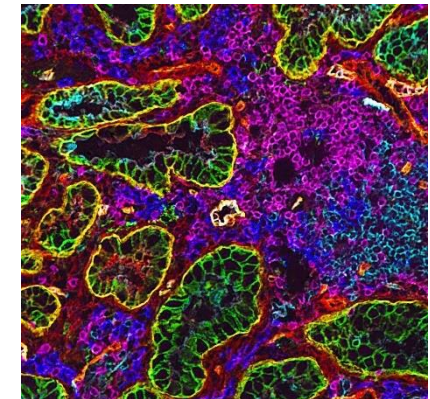
- Tedious analysis
- In some cancers (e.g. prostate) < 1% of the image is cancer-related
- For some cancers, it does not allow precise diagnostics (e.g. some astrocytomas vs oligodendrogliomas)
- Gives non-structured data

Immunohistochemistry (IHC)

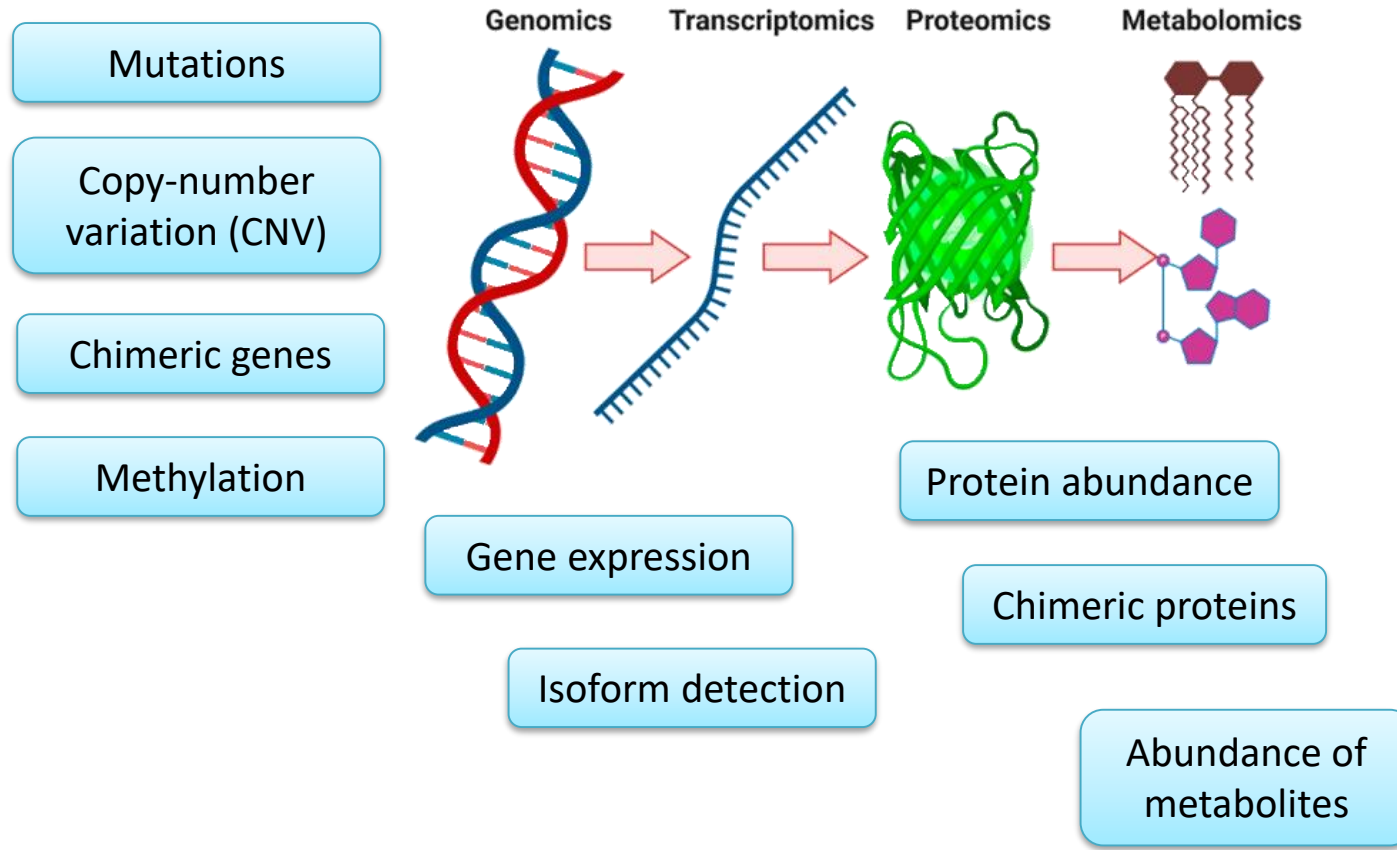


Ki-67 - proliferation marker

Multicolor IHC



Invasive Approach 2: Molecular Profiling



Features of molecular approach

- Very specific
- Generate a lot of data
- Generate structured data

Issues of molecular approach

- Quite expensive
- Is sensitive to heterogeneity of samples
- Is sensitive to a technique

a Reference cohort (91 classes)

Embryonal

- 1 ETMR
- 1 MB, WNT
- 2 MB, G3
- 2 MB, G4
- 2 MB, SHH CHL AD
- 2 MB, SHH INF
- 2 ATRT, MYC
- 2 ATRT, SHH
- 2 ATRT, TYR
- 2 CNS NB, FOXR2
- 5 HGNET, BCOR

Glioblastoma

- 1 DMG, K27
- 2 GBM, G34
- 2 GBM, MES
- 2 GBM, RTK I
- 2 GBM, RTK II
- 2 GBM, RTK III
- 2 GBM, MID
- 2 GBM, MYCN

Glio-neuronal

- 1 CN
- 1 DLGNT
- 1 LIPN
- 1 LGG, DIG/DIA
- 1 LGG, DNT
- 1 LGG, RGNT
- 1 RETB
- 2 ENB, A
- 2 ENB, B
- 2 PGG, NG
- 4 LGG, GG

Sella

- 1 CPH, ADM
- 1 CPH, PAP
- 1 PITAD, ACH
- 1 PITAD, FSH LH
- 1 PITAD, PRL
- 1 PITAD, STH SPA
- 1 PITAD, TSH
- 2 PITAD, STH DNS A
- 2 PITAD, STH DNS B
- 4 PITUI, SCO, GCT

Ependymal

- 1 EPN, RELA
- 2 EPN, YAP
- 2 EPN, PF A
- 2 EPN, PF B
- 2 EPN, SPINE
- 4 EPN, MPE
- 4 SUBEPN, PF
- 4 SUBEPN, SPINE
- 4 SUBEPN, ST

Other glioma

- 1 CHGL
- 1 LGG, SEGA
- 2 LGG, PA PF
- 2 LGG, PA MID
- 5 ANA PA
- 5 HGNET, MN1
- 5 IHG
- 4 LGG, MYB
- 4 LGG, PA/GG ST
- 4 PXA

Nerve

- 1 SCHW
- 1 SCHW, MEL

Pineal

- 2 PTPR, A
- 2 PTPR, B
- 2 PIN T, PB B
- 4 PIN T, PB A
- 3 PIN T, PPT

Mesenchymal

- 1 EWSDM
- 1 CHORD
- 1 HMB
- 4 MNG
- 3 SFT HMPG
- 5 EFT, CIC

Melanocytic

- 1 MELAN
- 1 MELCYT

Plexus

- 3 PLEX, AD
- 3 PLEX, PED A
- 3 PLEX, PED B

Glioma IDH

- 3 A IDH
- 3 A IDH, HG
- 3 O IDH

Glioma IDH

- 1 LYMPHO
- 1 PLASMA

Haematopoietic

- ADENOPTIT
- WM
- CEBM
- HEMI
- HYPTHAL
- INFLAM
- PINEAL
- PONS
- REACT

Control

- 1 LGG, DIG/DIA
- 2 SCHW, MEL
- 3 SUBEPN, SPINE
- 4 LGG, MYB
- 5 IHG
- 6 LGG, PA/GG ST
- 7 LGG, GG
- 8 DLGNT
- 9 LGG, SEGA
- 10 Control REACT

Relation to WHO entitles (category):

- 1 Equivalent
- 2 Subclass
- 3 Not equivalent (combining grades)
- 4 Not equivalent (combining entitles)
- 5 Not recognized by WHO

b *t*-SNE dimensionality reduction (2,801 samples)

1 LGG, DIG/DIA
2 SCHW, MEL
3 SUBEPN, SPINE
4 LGG, MYB
5 IHG
6 LGG, PA/GG ST
7 LGG, GG
8 DLGNT
9 LGG, SEGA
10 Control REACT

Capper et al. *Acta Neuropathologica* 2018, 136:181

b

Cross-validation

Predicted

Annotated

Samples in annotated class (%)

0 50 100

MCF MB, G3/4

MCF MB, SHH

MCF ENB

MCF LGG, PA

MCF PLEX

MCF GLM, IDH

MCF ATRT

MCF glioblastoma, IDH wild-type

MYC

SHH

TYR

RTK III

RTK II

RTK I

MYCN

MID

MES

d

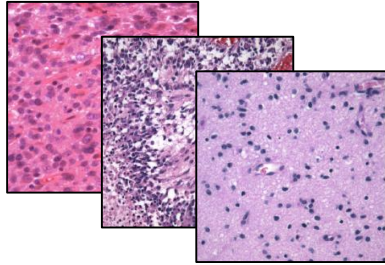
DNA methylation class: diffuse leptomeningeal glioneuronal tumor (score 0.99)

Copy number profile: 1p loss among other changes

1 2 3 4 5 6 7 8 9 10 11 12 13 14 15 16 17 18 19 20 21 22 X Y

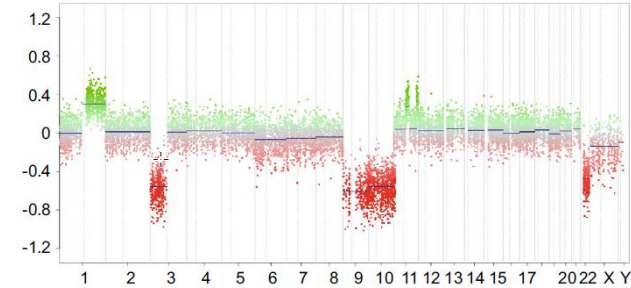
- Methylation showed more specificity than histopathology identifying types of brain tumors
- Highly standardized pipeline allowed analysis across many cohorts
- **Result:** "Heidelberg classifier" is used by pathologists 😊

1. Histopathology



- Automate analysis
- Transform unstructured data (images) to structured (features)

2. Molecular methods

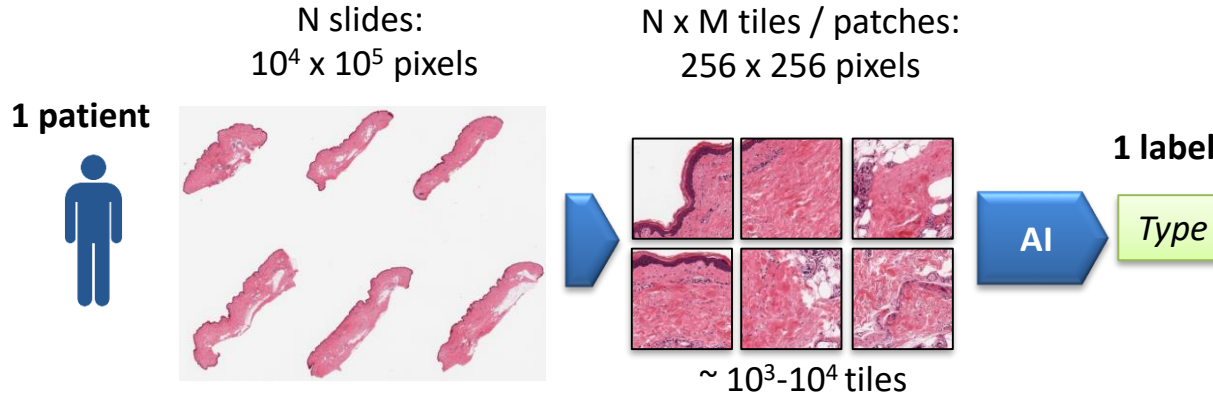


- Deconvolute mixed signals
- Integrate various molecular data

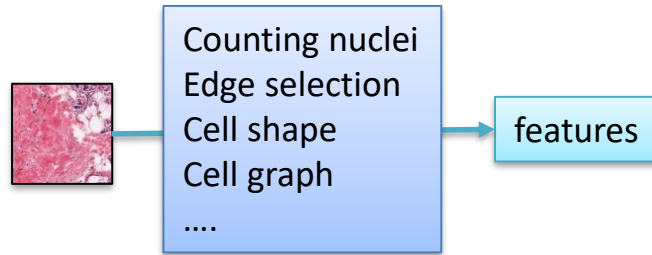
Integrate both approaches for better patient diagnostics and studying molecular processes

1. Digital Histopathology and Feature Extraction

The Task

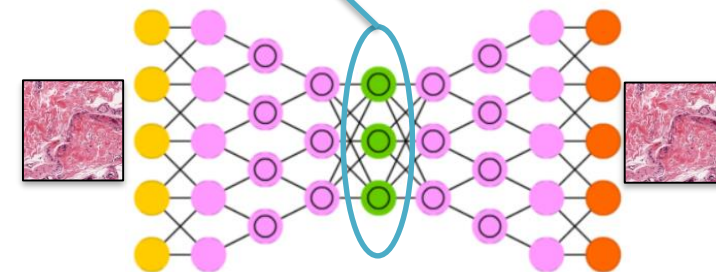
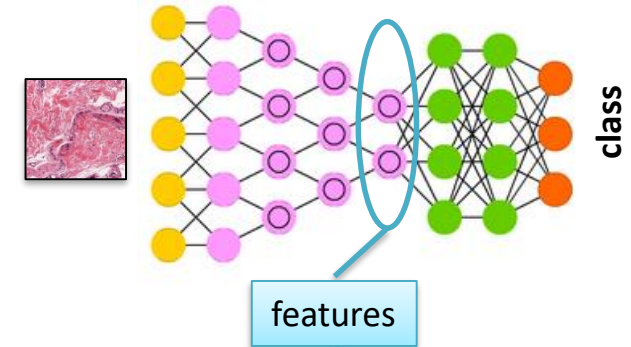


Classical image analysis approaches

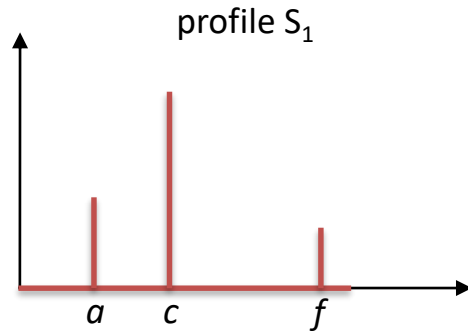


Deep Artificial Neural Networks

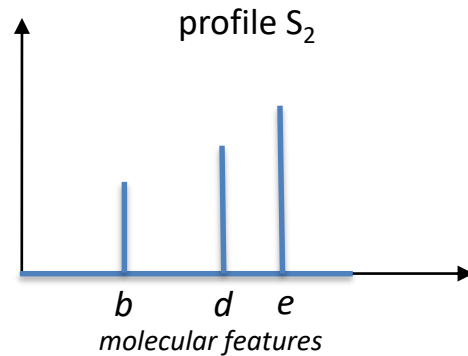
Deep convolutional neural network (CNN)



2. Deconvolution: Concept



$$X = S \times M$$

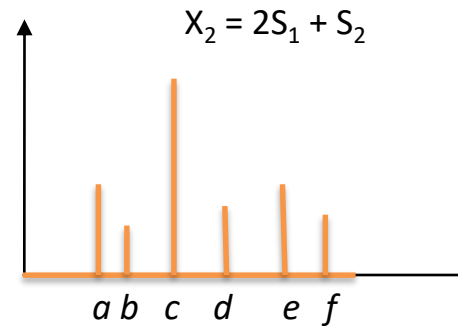
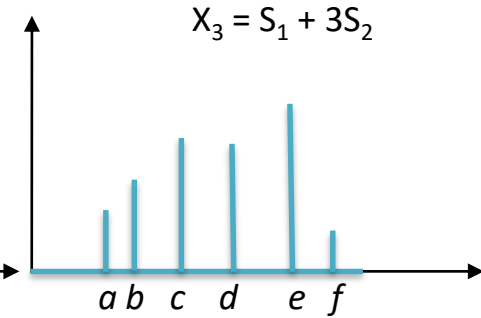
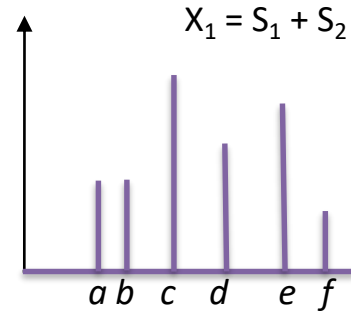


$M =$

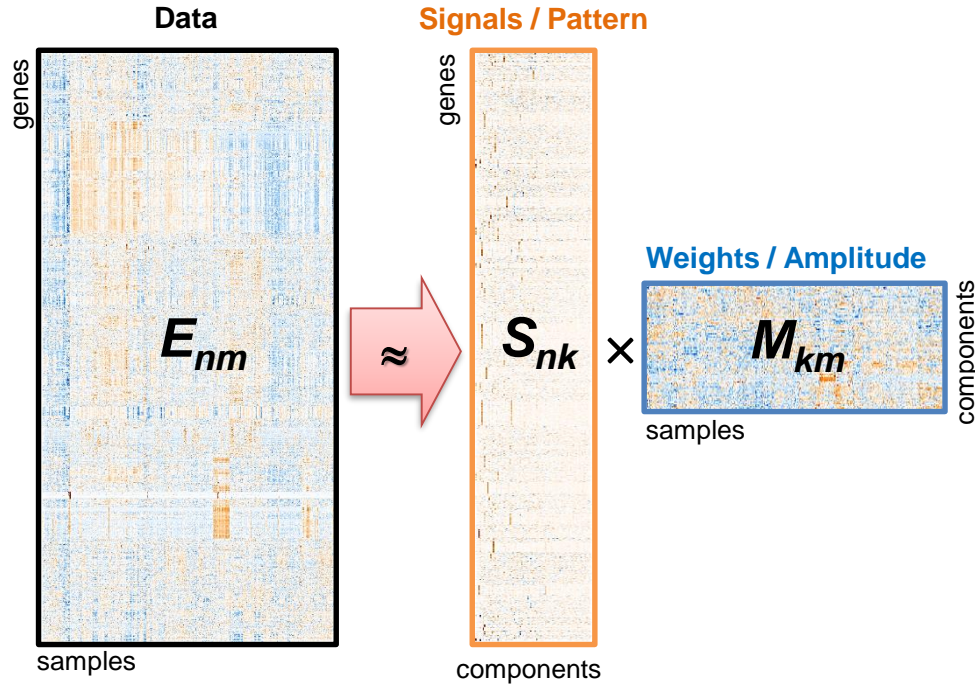
1	2	1
1	1	3



Often called:
- **decomposition**
- **deconvolution**

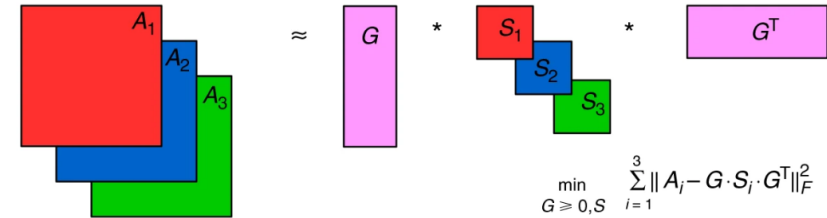


Deconvolution via Matrix Factorization



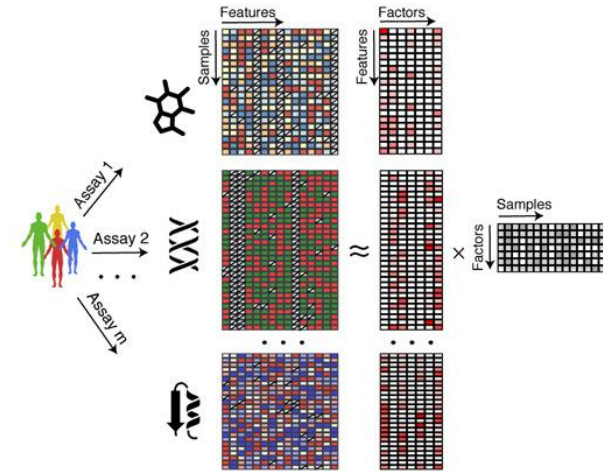
PCA: principal component analysis
NMF: non-negative matrix factorization
ICA: independent component analysis
etc.

Matrix tri-factorization



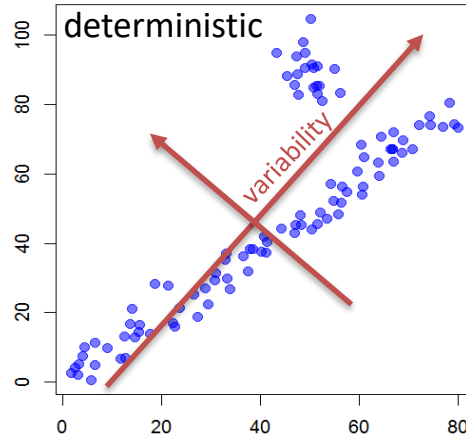
Malod-Dognin et al. *Nat Commun* 2019, 10:805

Multi-omics Factor Analysis



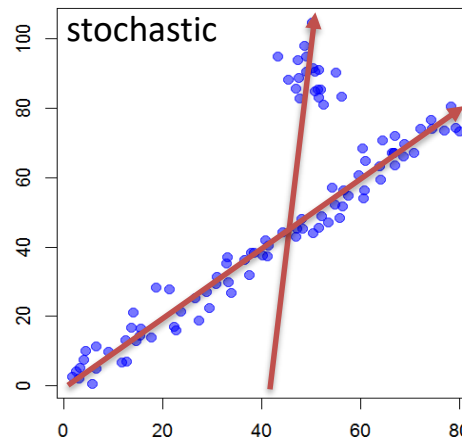
Argelaguet et al. *Mol Syst Biol* 2018, 14:e8124

PCA



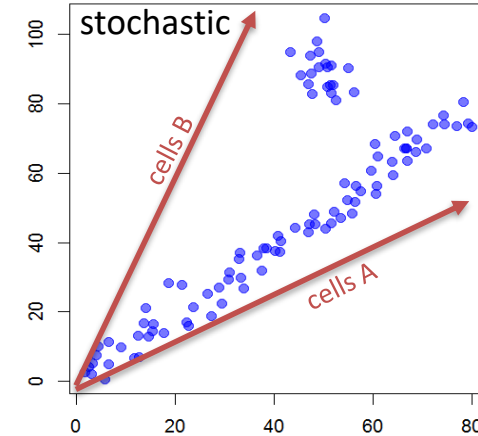
- + deterministic & fast
- + any number of samples
- + unsupervised
- often biological factors are presented by a sum of several components
- positive and negative values

ICA



- + **correlates with biology**
- + **unsupervised (agnostic)**
- + **quite stable**
- stochastic
- needs a lot of samples
- positive and negative values

NMF

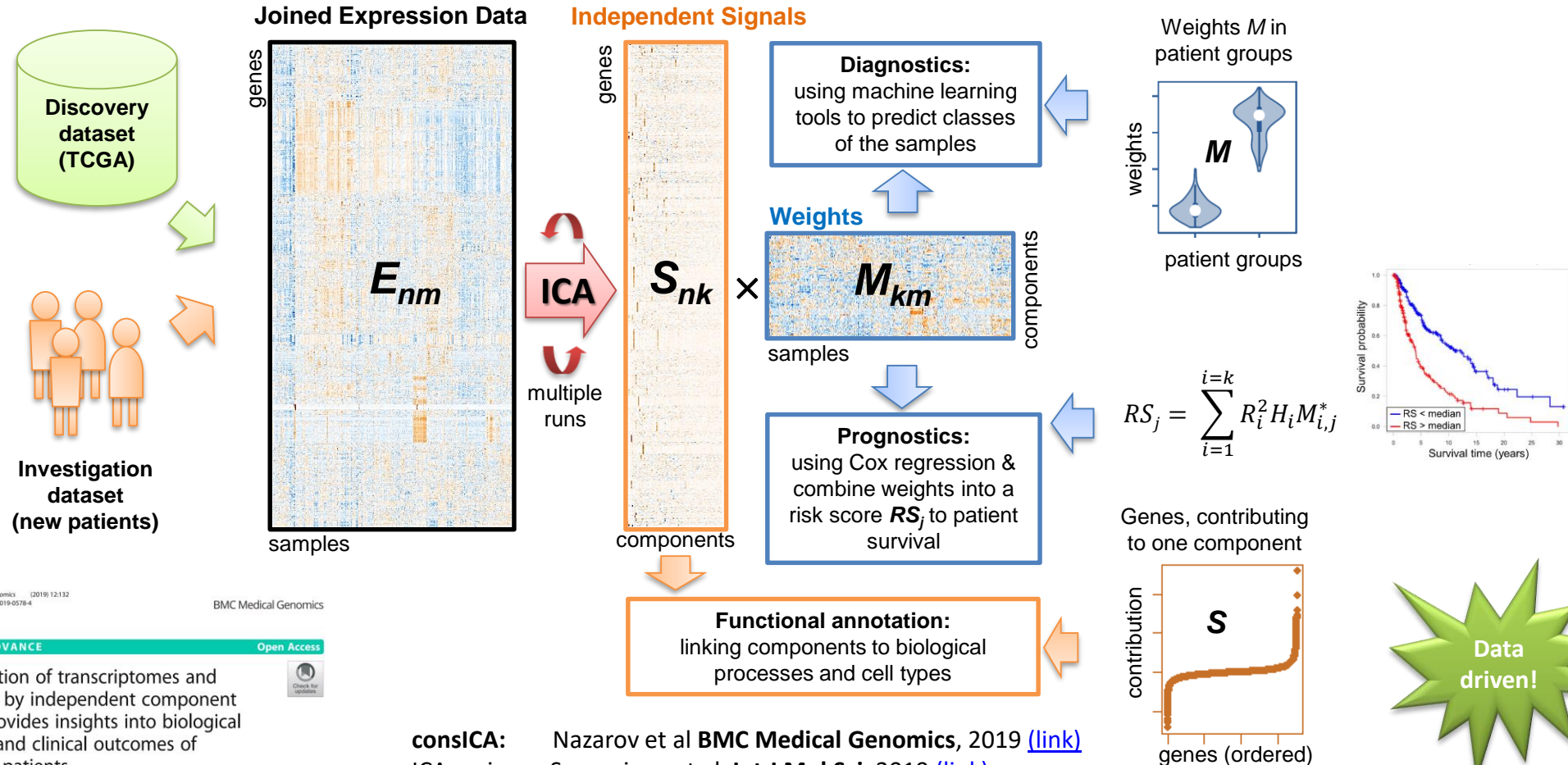


- + semi-unsupervised
- + easy to interpret
- stochastic
- unstable

Sompairac et al, Int J Mol Sci, 2019 ([link](#))

Cantini et al, Bioinformatics, 2019 ([link](#))

Research Focus: Deconvolution of Omics Data



Nazarov et al. BMC Medical Genomics
https://doi.org/10.1186/s12920-019-0578-4

BMC Medical Genomics

TECHNICAL ADVANCE Open Access

Deconvolution of transcriptomes and miRNomes by independent component analysis provides insights into biological processes and clinical outcomes of melanoma patients

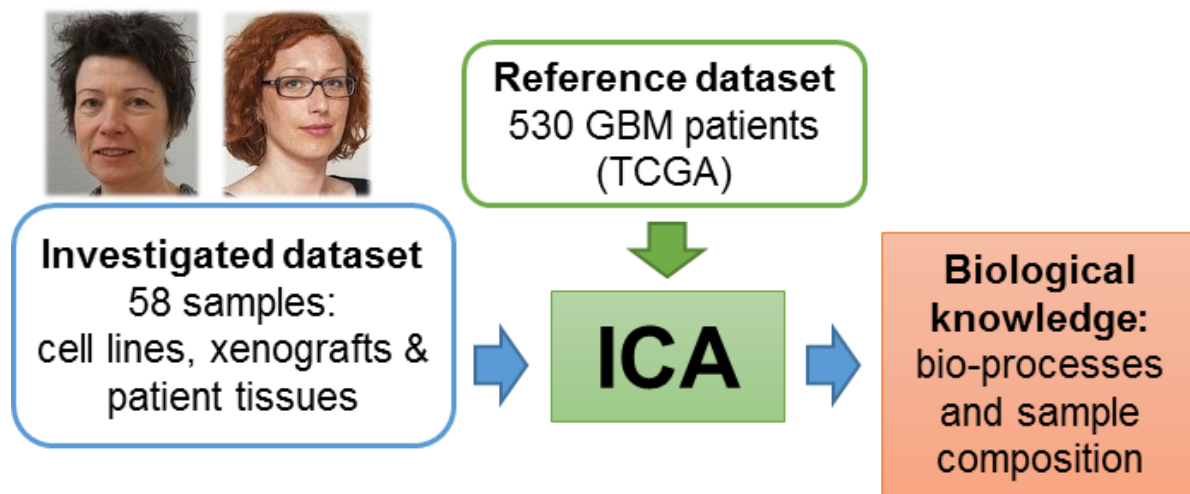
Petr V. Nazarov^{1*}, Anke K. Wienecke-Baldacchino^{2,3†}, Andrei Zinovyev^{4,5}, Ursula Czerwiska^{4,5,6}, Arnaud Muller⁴, Dorothee Nashan⁴, Gunnar Dittmar⁴, Francisco Azuaje¹ and Stephanie Kreis²

consICA: Nazarov et al **BMC Medical Genomics**, 2019 ([link](#))

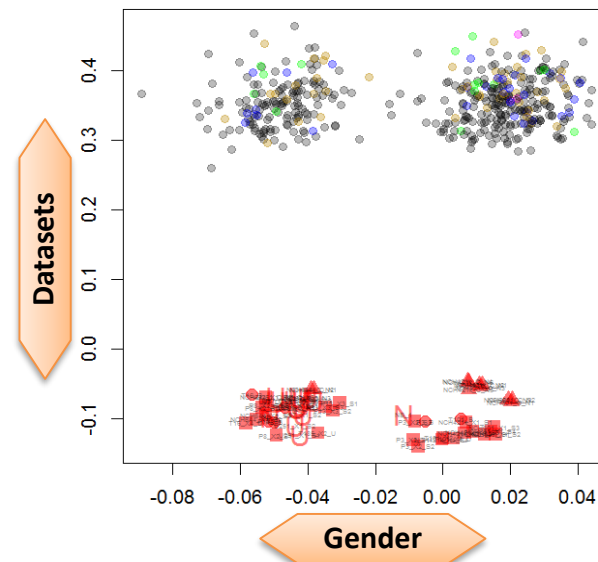
ICA review: Sompairac, et al **Int J Mol Sci**, 2019 ([link](#))

Application: Golebiewska et al, **Acta Neuropathol**, 2020

Scherer, Nazarov et al, **Nat Protoc**, 2020



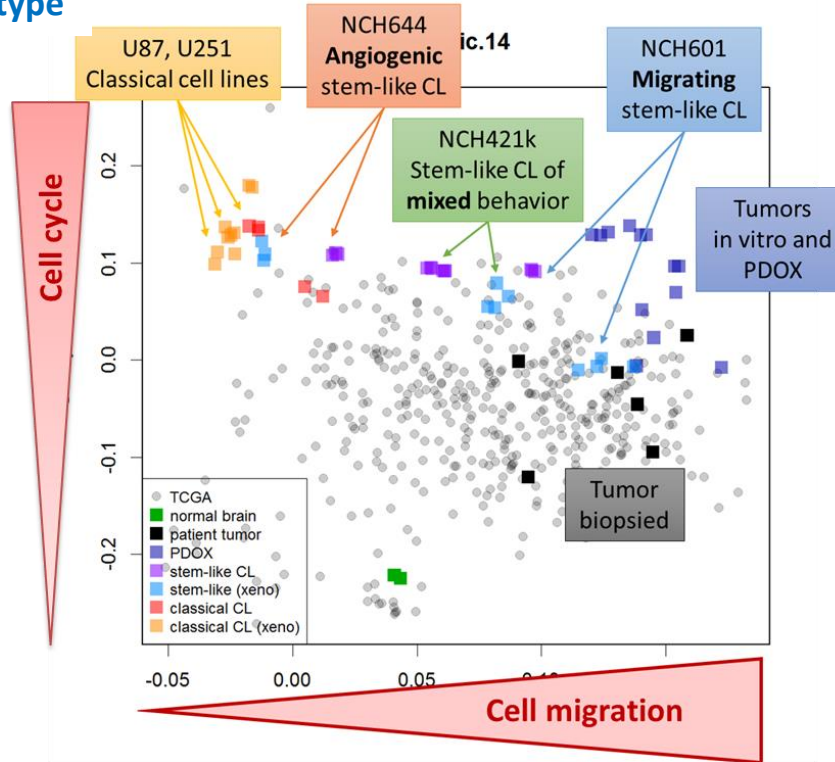
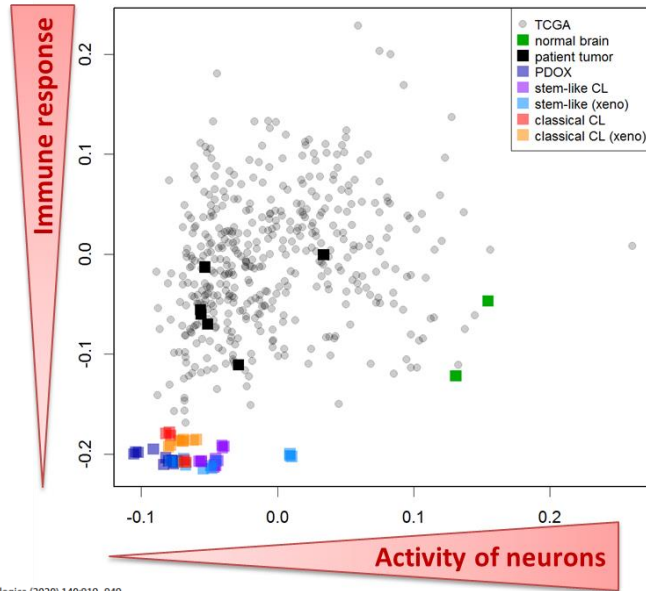
Technical/trivial components:
gender and platforms



- We were able to map in-house cell line data onto TCGA dataset (GBM)
- Some components captured *technical factors* → (and thus clean other components from them)
- Other – relevant *biological information*: cell cycle, cell migration, presence of stromal and immune cells. **We were able to predict phenotype of cell lines using their transcriptomes.**

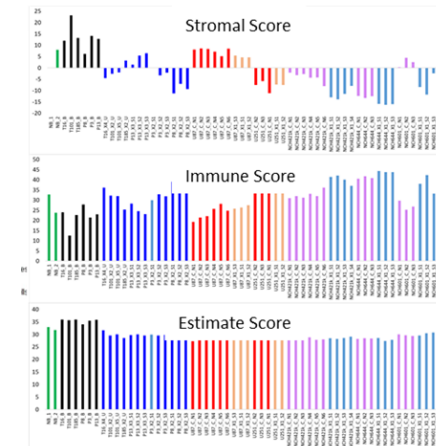
GBM Cell Lines

ICA correctly predicts sample composition & phenotype



- ICA deconvolution is reasonable and predicts phenotypic behavior of cell lines
- Tumor cells show higher mobility in xenografts

ESTIMATE was confused



Golebiewska A. et al, *Acta Neuropathologica*, 2020 ([link](#))

Phenotype of cell lines were predicted using unsupervised deconvolution of their transcriptomes!

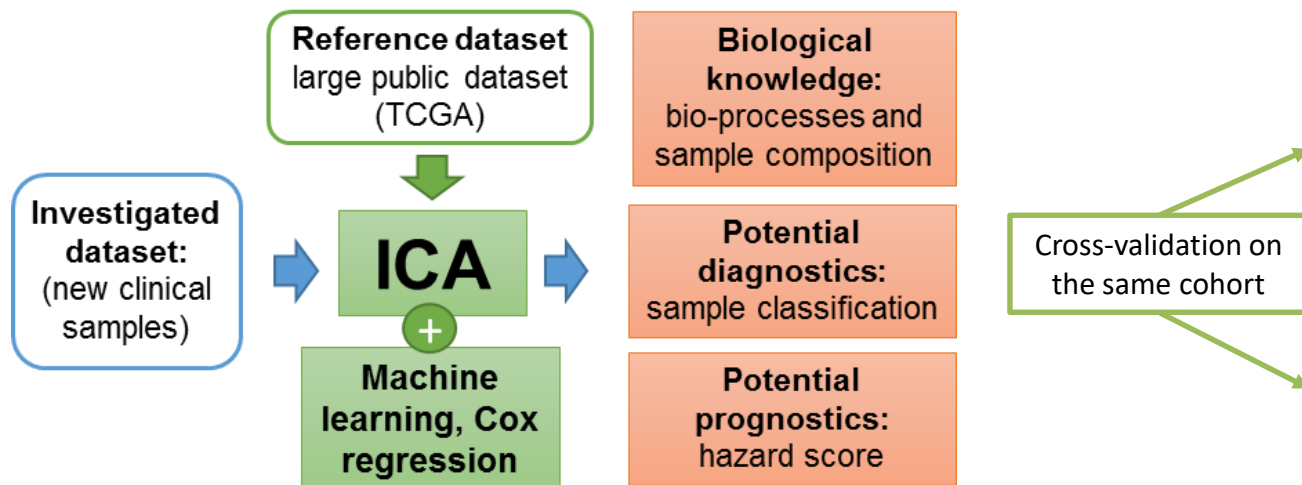
Acta Neuropathologica (2020) 140:919–949
<https://doi.org/10.1007/s00401-020-02226-7>

ORIGINAL PAPER

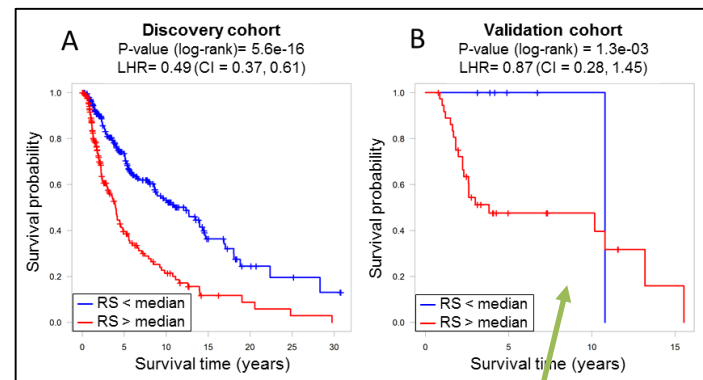


Patient-derived organoids and orthotopic xenografts of primary and recurrent gliomas represent relevant patient avatars for precision oncology

Anna Golebiewska¹ · Ann-Christin Hau¹ · Anaïs Oudin¹ · Daniel Stieber^{1,2} · Yahaya A. Yabo^{1,3} · Virginie Baus¹ · Vanessa Barthelemy¹ · Eliane Klein¹ · Sébastien Bougnaud¹ · Olivier Keunen^{1,4} · May Wantz¹ · Alessandro Michelucci^{1,5,6} · Virginie Neirinx¹ · Arnaud Muller⁴ · Tony Kaoma⁶ · Petr V. Nazarov⁴ · Francisco Azuaje⁴ · Alfonso De Falco^{2,3,7} · Ben Flies⁴ · Lorraine Richart^{3,7,8,9} · Suresh Poovathingal⁶ · Thais Arns⁶ · Kamil Grzyb⁶ · Andreas Mock^{10,11,12,13} · Christel Herold-Mende¹⁰ · Anne Steino^{14,15} · Dennis Brown^{14,15} · Patrick May⁶ · Hrvoje Miletic^{16,17} · Tathiane M. Malta¹⁸ · Houtan Noushmehr¹⁸ · Yong-Jun Kwon⁹ · Winnie Jahn^{19,20} · Barbara Klink^{2,9,19,20,21} · Georgette Tanner²² · Lucy F. Stead²² · Michel Mittelbronn^{6,7,8,9} · Alexander Skupin⁶ · Frank Hertel^{6,23} · Rolf Bjerkgvig^{1,16} · Simone P. Niclou^{1,16}



Cluster			
Accuracy	Actual cluster		
90.0%	immune	keratine	MITF-low
immune	160	9	6
keratine	9	91	6
MITF-low	1	2	47



$$RS_j = \sum_{i=1}^{i=k} R_i^2 H_i M_{i,j}^*$$

j – patient index
 i – component index
 R_i^2 – stability of i -th component (from 0 to 1)
 H_i – Cox' log hazard ratio calculated on **training set**
 $M_{i,j}^*$ – element of centered & scaled M-matrix

Independent cohort,
different platform

- In addition to diagnostics and prognostics, ICA allowed ranking patients based on the activity of biological processes: cell cycle, signals of leukocytes, etc.

Deciphering biological processes and cell types

Cluster	Component	Risk (p-value)	Meaning	P2PM	P4PM	P6PM	P4NS	NHEM
Immune	RIC2	decreased (1.8e-4)	B cells	0.11	0.07	0.02	0.19	0.01
	RIC25	decreased (2.8e-7)	T cells	0.26	0.06	0.24	0.18	0.00
	RIC27	no effect	B cells	0.80	0.37	0.31	0.80	0.00
	RIC28	no effect	response to wounding	0.34	0.57	0.78	0.43	0.84
	RIC37	no effect	IFN signalling pathway	0.97	0.66	0.99	0.90	1.00
	RIC57	no effect	monocytes	0.00	0.25	0.24	0.02	0.00
Stromal and angiogenic	MIC20	decreased (1.2e-4)	T cells, chr1q32.2	0.14	0.08	0.37	0.02	0.19
	RIC13	no effect	cells of stroma	0.81	0.40	0.50	0.86	0.03
	RIC49	no effect	endothelial cells	0.73	0.12	0.29	0.84	0.00
	MIC22	no effect	miR-379/miR-410 cluster, chr14q32.2, 14q32.31	0.29	0.20	0.27	0.38	0.16
Skin-related	MIC25	no effect	stromal cells; clusters: chr1q24.3, 5q32, 17p13.1, 21q21.1	0.97	0.85	0.76	0.80	0.26
	RIC5	increased (5.8e-3)	epidermis development and keratinisation	0.92	0.93	0.96	0.92	0.87
	RIC7	increased (8.9e-6)	epidermis development and keratinisation	0.94	0.93	0.93	0.95	0.57
	RIC19	increased (4.0e-2)	epidermis development and keratinisation	1.00	0.62	0.22	1.00	0.93
	RIC31	increased (2.2e-2)	epidermis development and keratinisation	0.98	0.85	0.89	0.99	0.28
	MIC9	increased (2.9e-2)	skin-specific miRNAs	0.95	0.88	0.87	0.91	0.83
Melanocytes	RIC4	increased (5.4e-3)	melanin biosynthesis	0.62	0.77	1.00	0.21	0.96
	RIC16	decreased (5.1e-4)	melanosomes (negative gene list)	0.68	0.77	0.54	0.75	0.39
	MIC11	no effect	potential regulators of malignant cells, chrXq27.3	0.21	0.96	0.62	0.13	0.48
	MIC14	decreased (1.5e-2)	potential regulators of melanocytes, chrXq26.3	0.01	0.29	0.67	0.29	0.38
Other	RIC55	increased (3.0e-2)	cell cycle	0.48	0.46	0.88	0.00	0.53
	RIC6	decreased (5.5e-3)	potentially linked to neuron differentiation	0.43	0.73	0.59	0.46	0.01
	MIC1	increased (9.4e-4)	regulators of EMT	0.11	0.07	0.02	0.19	0.01

ESTIMATE

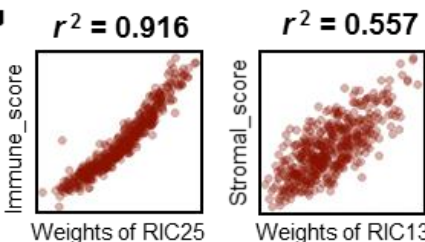
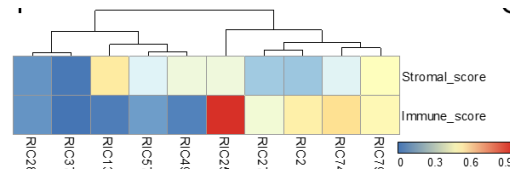


Article | OPEN | Published: 11 October 2013

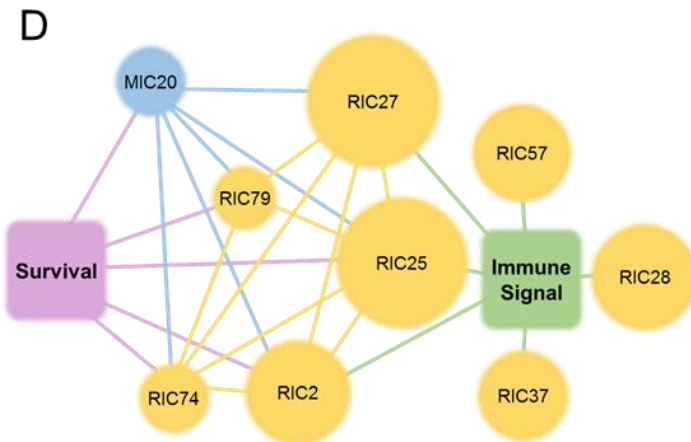
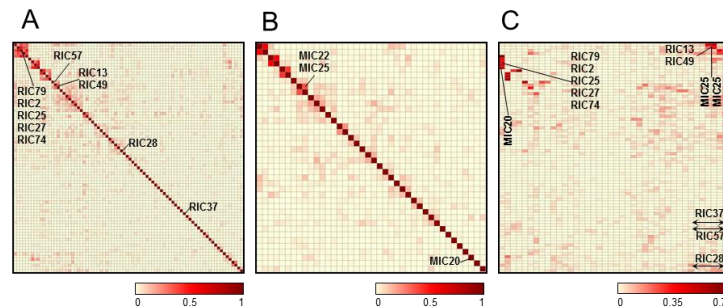
Inferring tumour purity and stromal and immune cell admixture from expression data

Kosuke Yoshihara, Maria Shahmoradgoli, Emmanuel Martinez, Rahulsham Vegesna, Hoon Kim, Wandaliz Torres-Garcia, Victor Treviño, Hui Shen, Peter W. Laird, Douglas A. Levine, Scott L. Carter, Gad Getz, Katherine Stemke-Hale, Gordon B. Mills & Roel G.W. Verhaak

Nature Communications 4, Article number: 2612 (2013) | Download Citation



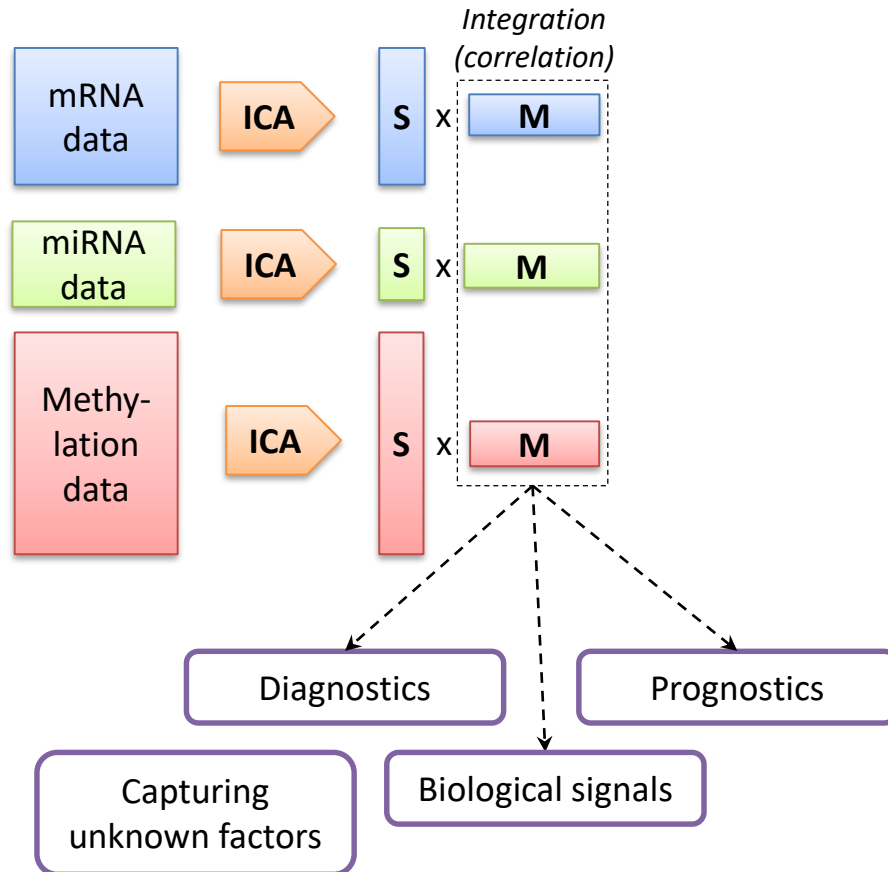
Data integration: mRNA + miRNA + ...



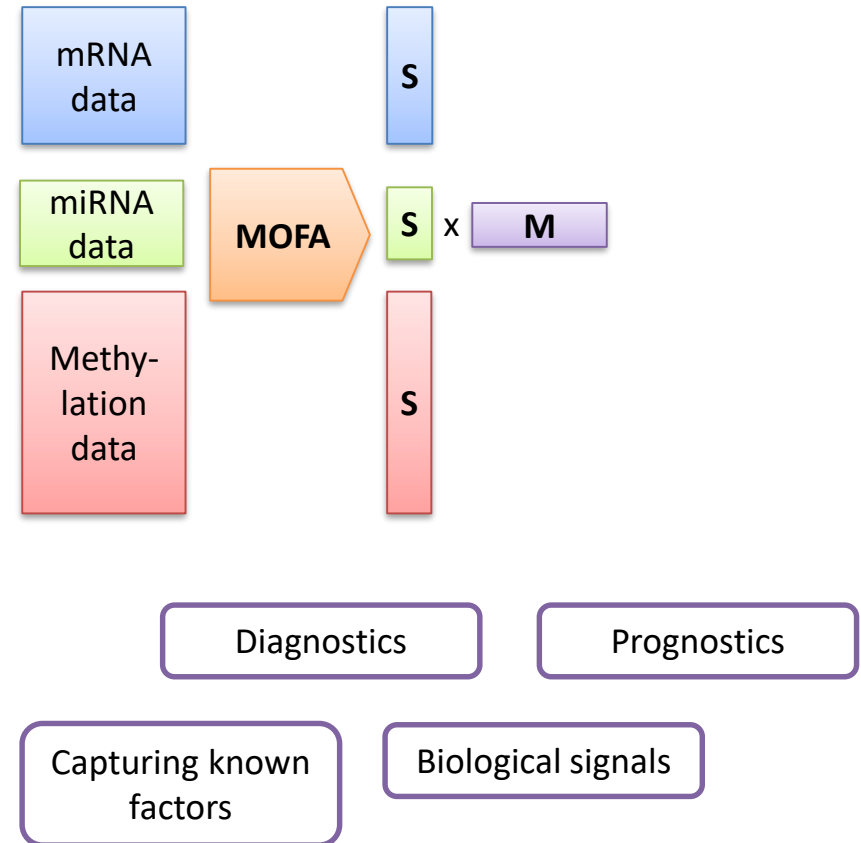
← New samples are mapped to the space defined by reference data.

Multi-omics Data Integration via Deconvolution

ICA: independent runs



MOFA: simultaneous analysis

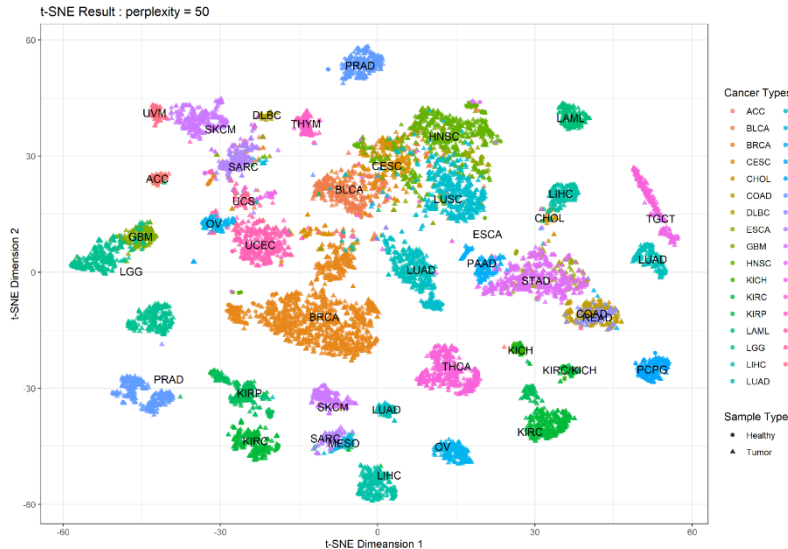


TCGA

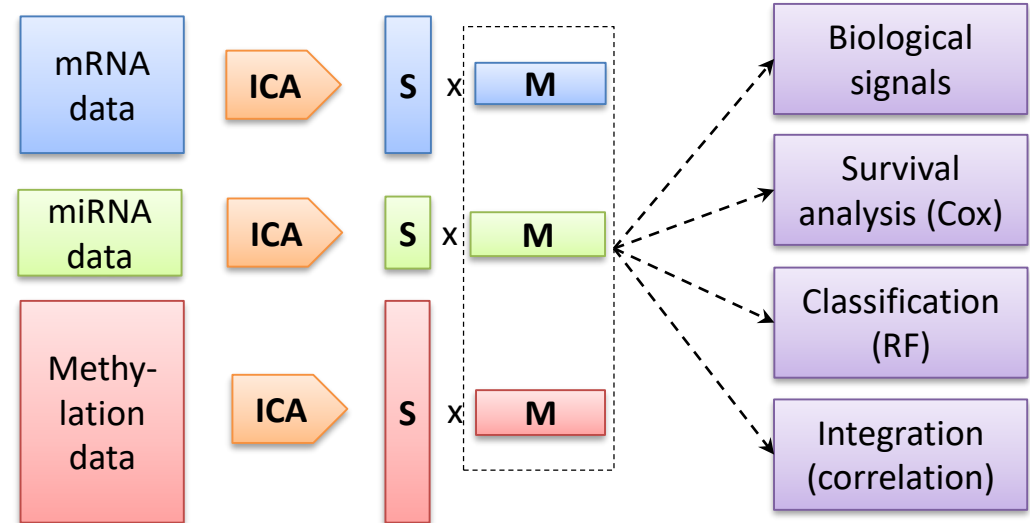
The Cancer Genome Atlas

>11k patients, 33 types of tumors

- **clinical data** (age, gender, survival...)
- **mRNA** (10k samples, 20k features)
- **miRNA** (> 9k samples, ~1k features)
- **methylation** (>9k samples, 450k features)



Approach

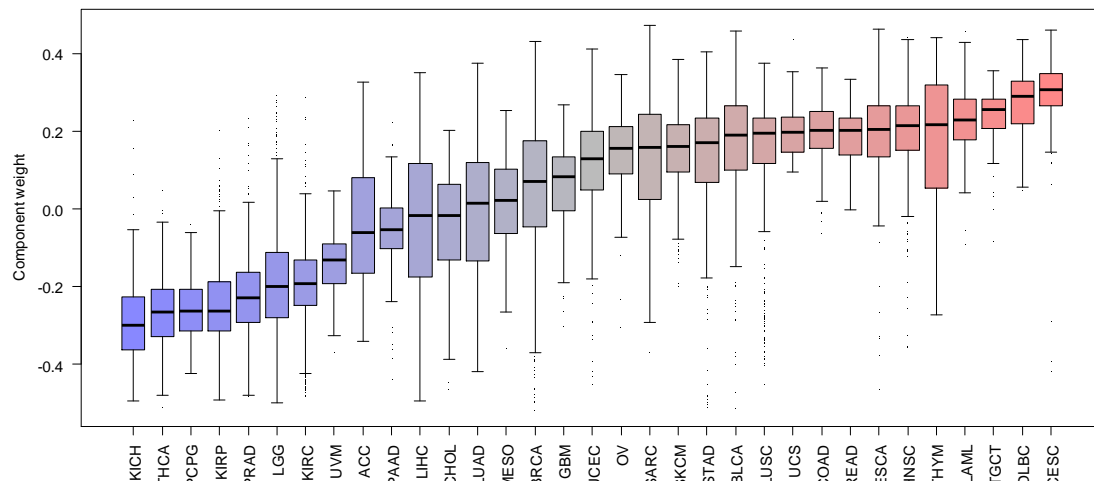


Here we used *consICA* with 100 components & 40 runs

Pan-cancer: ICA Components

ICA Results: Cell Cycle

RIC27: Mitotic Cell Cycle



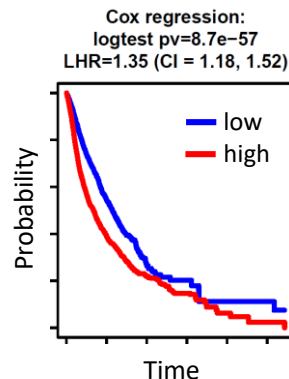
prostate
adenocarcinoma

low grade
glioma

glioblastoma
(IDHwt)

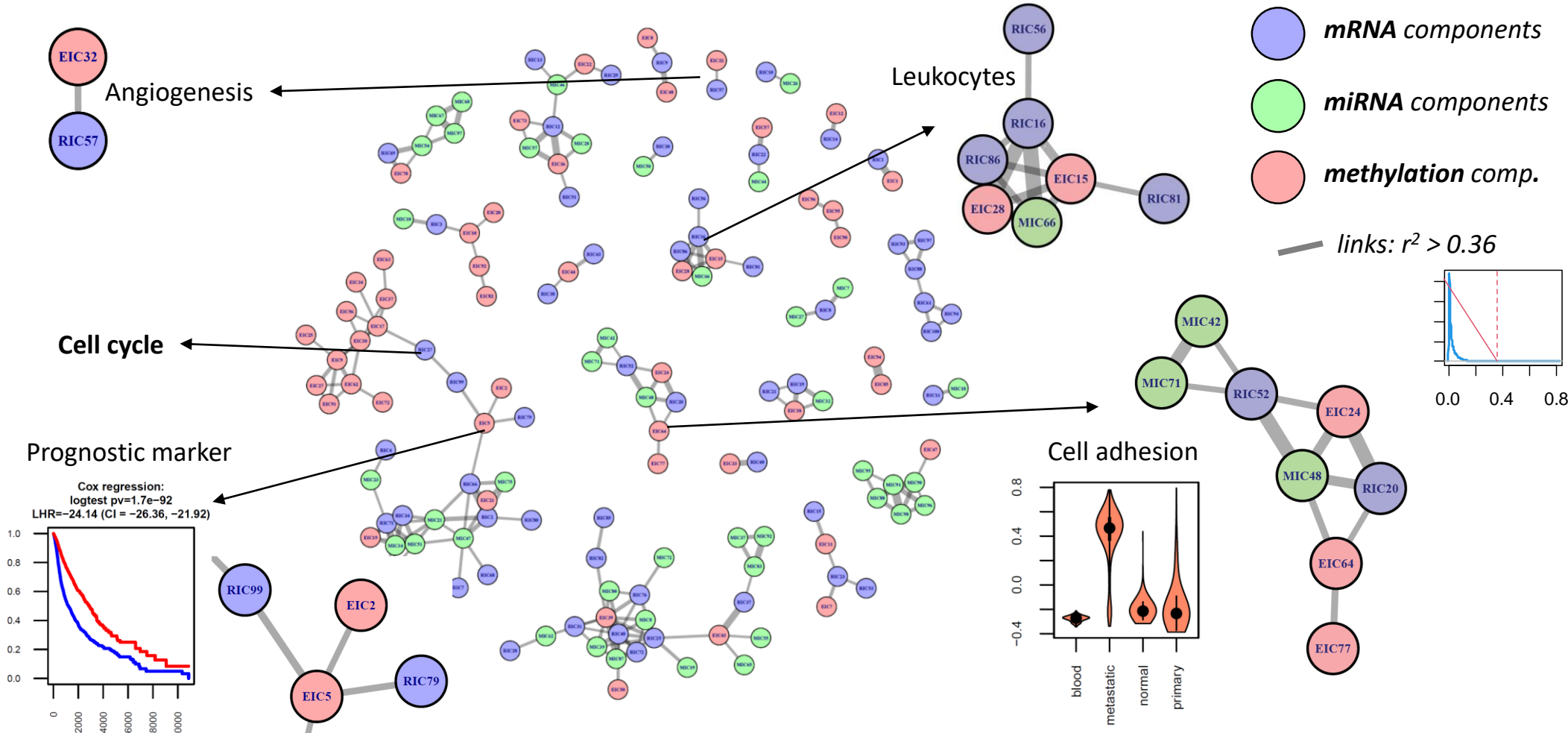
diffuse
lymphoma

cervical s.c.c &
endoservical a.c.



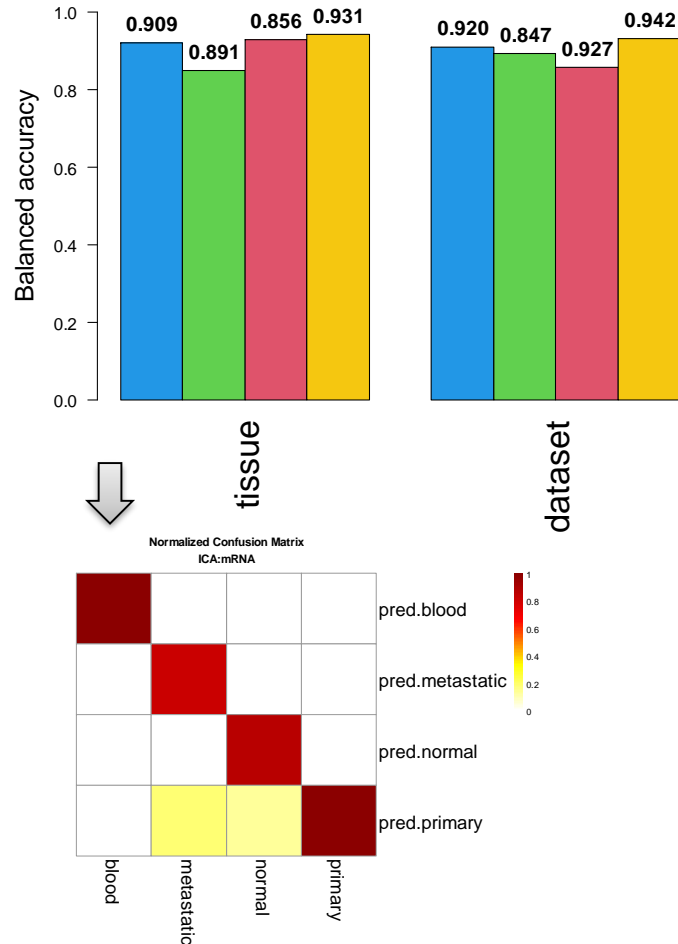
Code	Study Name
ACC	Adrenocortical carcinoma
BLCA	Bladder urothelial carcinoma
BRCA	Breast invasive carcinoma
CESC	Cervical sq. cell carcinoma and endocervical adenocarcinoma
CHOL	Cholangiocarcinoma
COAD	Colon adenocarcinoma
DLBC	Lymphoid neoplasm diffuse large b-cell lymphoma
ESCA	Esophageal carcinoma
GBM	Glioblastoma multiforme
HNSC	Head and neck squamous cell carcinoma
KICH	Kidney chromophobe
KIRC	Kidney renal clear cell carcinoma
KIRP	Kidney renal papillary cell carcinoma
LAML	Acute myeloid leukemia
LCML	Chronic myelogenous leukemia
LGG	Brain lower grade glioma
LIHC	Liver hepatocellular carcinoma
LUAD	Lung adenocarcinoma
LUSC	Lung squamous cell carcinoma
MESO	Mesothelioma
OV	Ovarian serous cystadenocarcinoma
PAAD	Pancreatic adenocarcinoma
PCPG	Pheochromocytoma and paraganglioma
PRAD	Prostate adenocarcinoma
READ	Rectum adenocarcinoma
SARC	Sarcoma
SKCM	Skin cutaneous melanoma
STAD	Stomach adenocarcinoma
TGCT	Testicular germ cell tumors
THCA	Thyroid carcinoma
THYM	Thymoma
UCEC	Uterine corpus endometrial carcinoma
UCS	Uterine carcinosarcoma
UVM	Uveal melanoma

Pan-cancer: ICA-based Data Integration



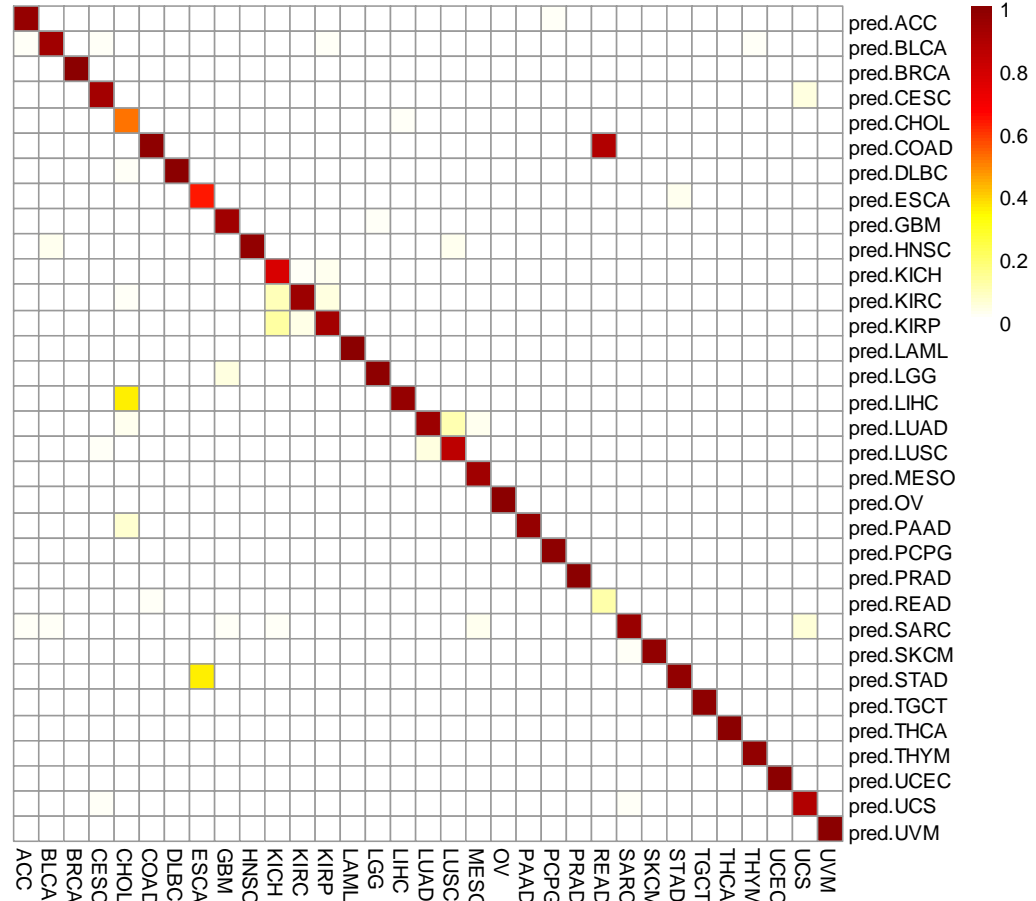
Pan-cancer: Classification

Classification by RF



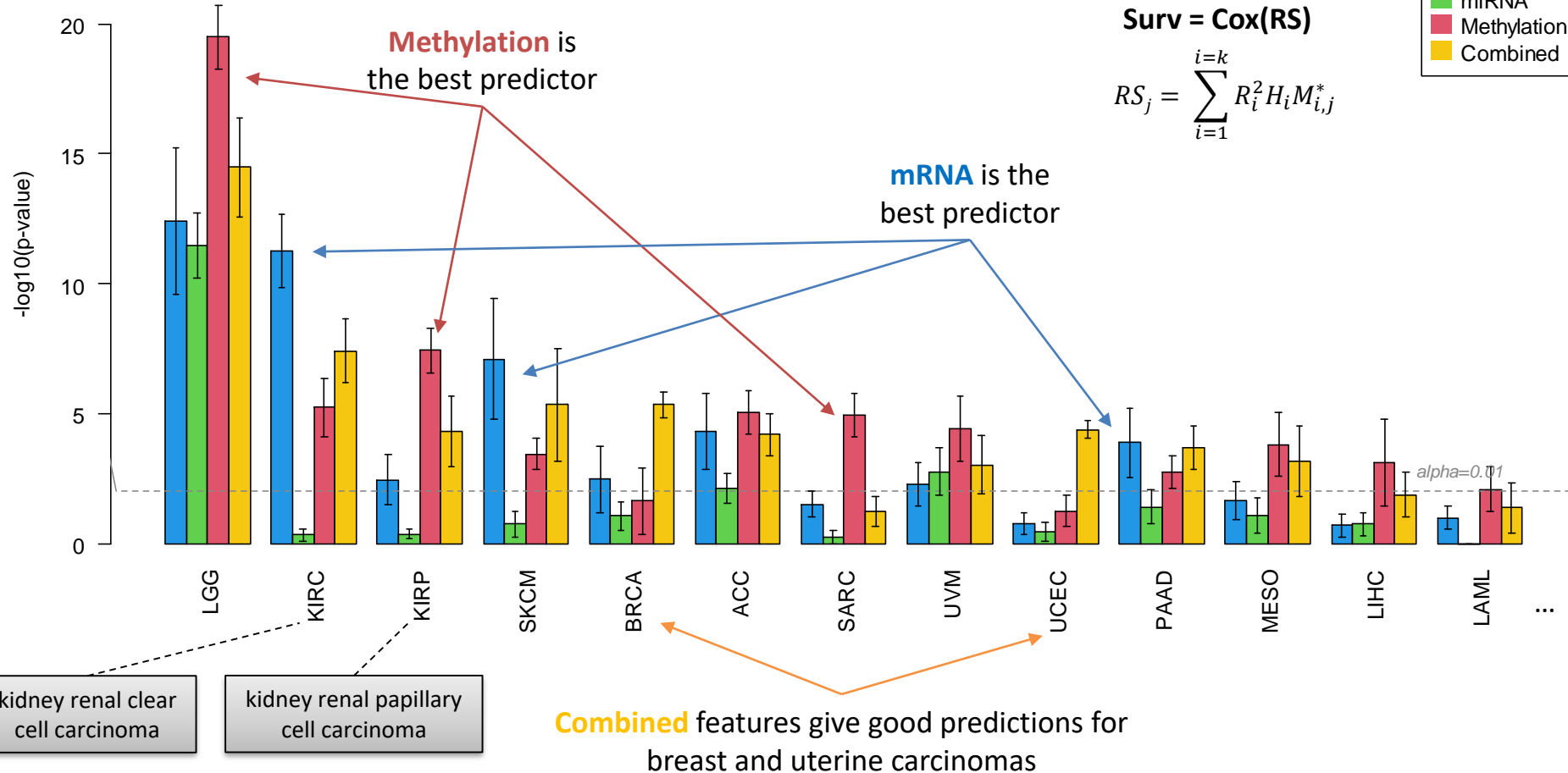
Normalized Confusion Matrix

ICA:mRNA



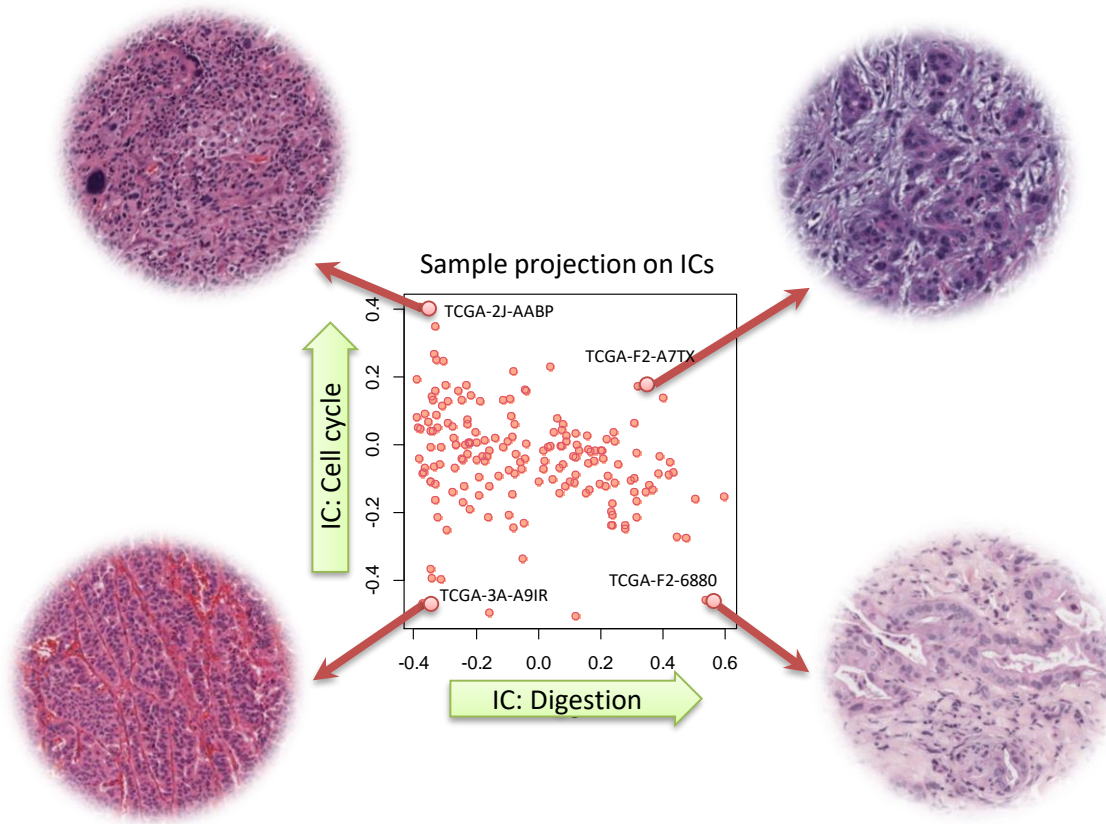
Pan-cancer: Prognosis

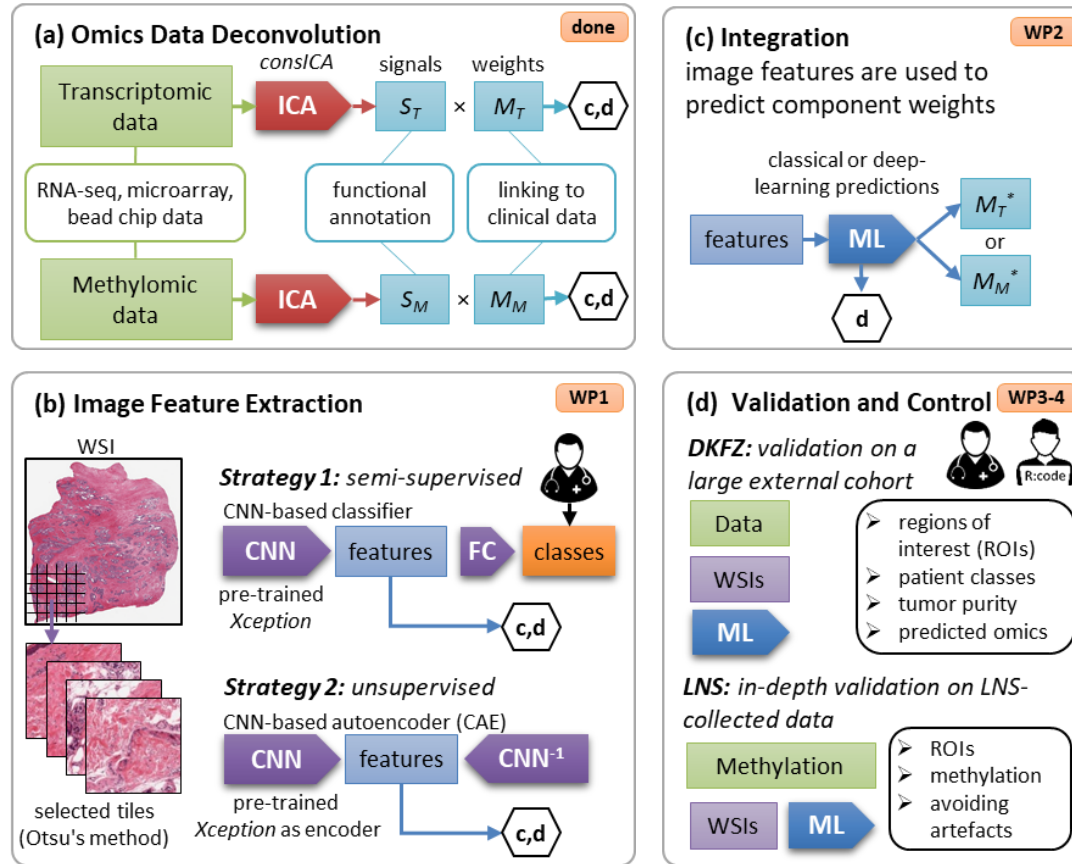
Prediction of survival (same cohort, cross-validation)



- ICA-based deconvolution:
 - Corrects **technical biases**
 - Extracts "cleaned" **biological signals** from bulk-sample data
 - **Maps new samples** into the space of biologically meaningful components
 - Extracts **prognostic features** and features with **classification** power
 - Can be used to **integrate** multi-omics data
 - **Diagnostic & prognostic** properties could be expected for many cancers
 - Reduce dimensionality
- Was validated:
 - Using acceptable computational methods (**cross-validation**)
 - On **cell lines**
 - **Independent cohorts** of patients

ICA results of mRNA expression data from TCGA-PAAD cohort





CAE: convolutional autoencoder; CNN: convolutional neural network; FC: fully-connected network or layer; ICA: independent component analysis; ML: machine learning; ROI: region of interest; WSI: whole slide image.

(a) Deconvolution of the omics data using developed tool *consICA*. This method was already developed and applied to entire GTEx (mRNA), TCGA (mRNA and meDNA), and DKFZ (mRNA) cohorts.

(b) Image analysis and feature extraction starts with a pre-trained *Xception* model and uses weakly supervised training to fine-tune model's parameters. Two strategies will be compared in the project: strategy 1 is a semi-supervised one using CNN-based classifier and strategy 2 – completely unsupervised using CAE. *Xception* will be used as an initial estimation of the encoder's parameters.

(c) Integration of ICA-weights and image features will be done either by a classical ML-approach (linear regression or random forest regression) or by a FC neural network.

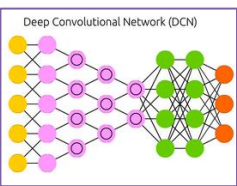
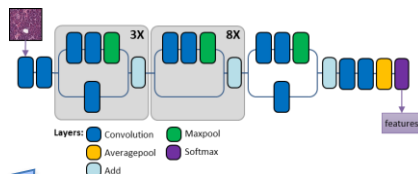
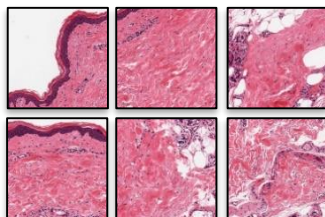
(d) A thorough validation of the results include (i) validation of an external pancreatic cancer cohort (DKFZ) and collection and (ii) in-depth analysis of in-house (LNS) samples of glioma patients. The expertise of the Co-PI (pathologist) will be used to validated predictions and the PI and his team will control that the WSI-features are sensible and not artefacts.

Preliminary Results

670+ patients 27 organs



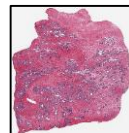
"normal" tissues



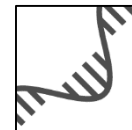
input

GTEX Data:

15k+ slides



17k+ RNA-seq



Sample:
1278 slides

zoom x10,
~10k x 10k px

480k tiles

256 x 256 px

Xception
model

Classification

Tile features

Slide features

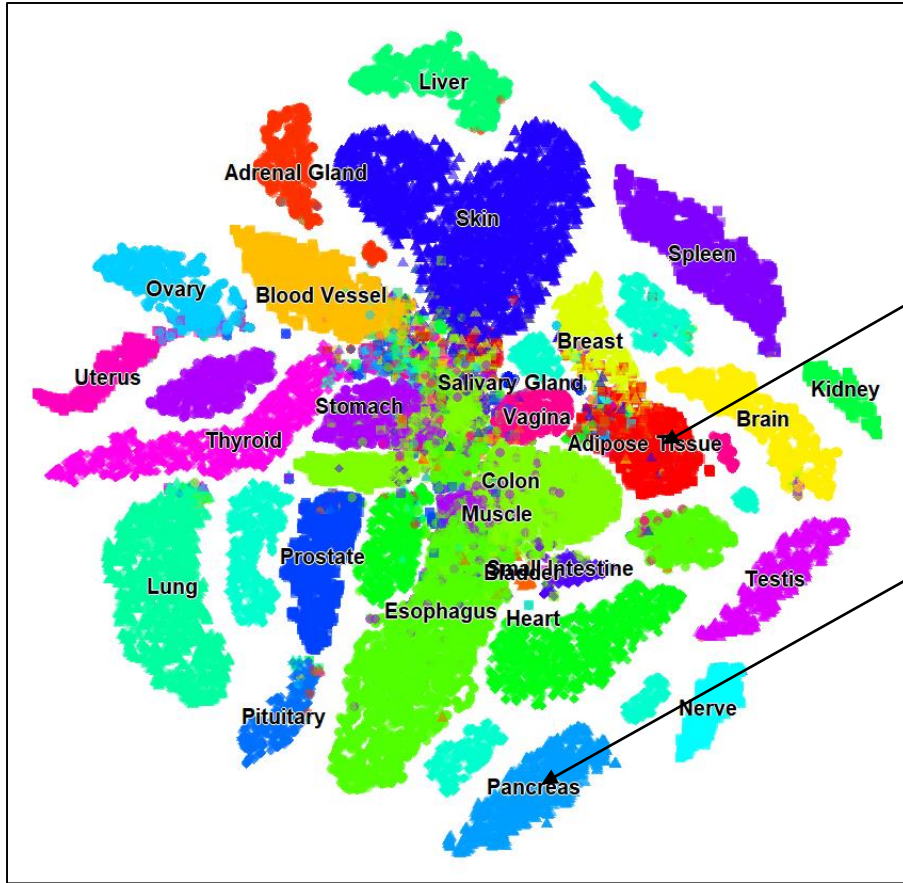
ICA

Functional
annotation
of ICs

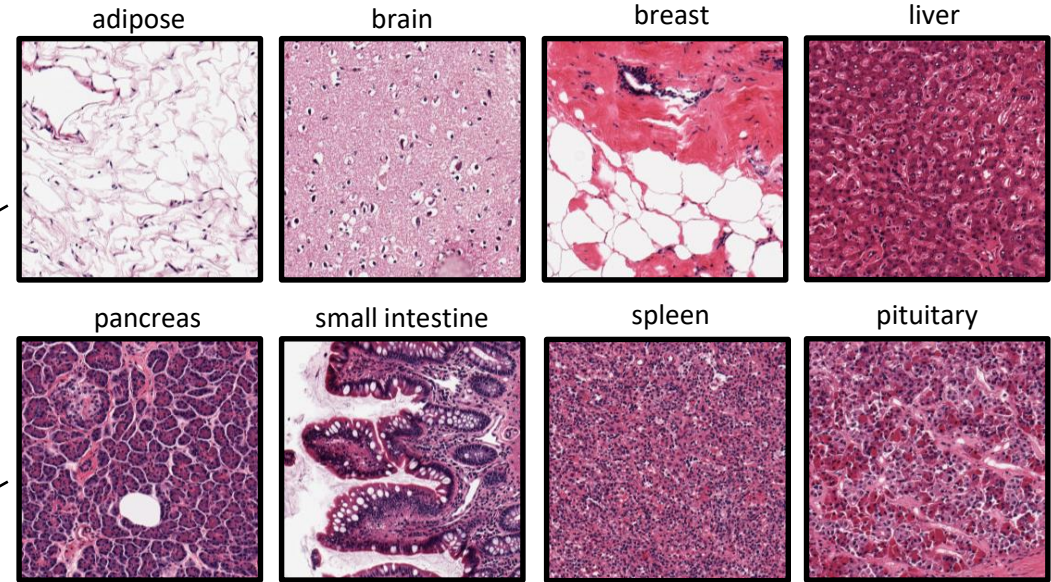
Weights of ICs

Integration &
predictions

output



Examples of tiles classified with top certainty and co-localized with class medoids



Xception, after parameter fine-tuning on organ classification task, transform each tile to ~150 non-zero features.

Further analysis:

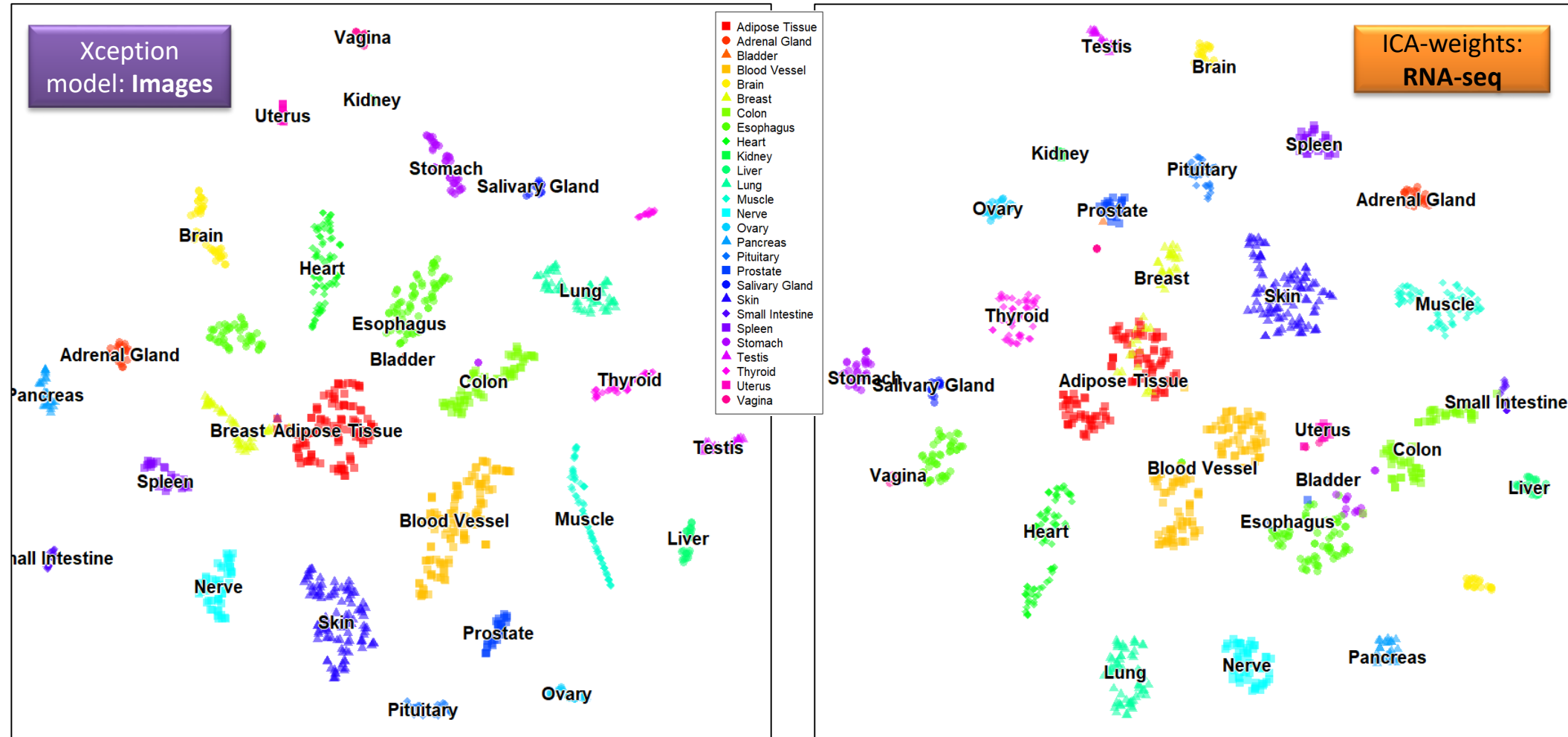
These features were summarized to slide-level. Only 50% top-correlated tiles were preserved (can be further improved later...)

Slide-level Analysis and ICA

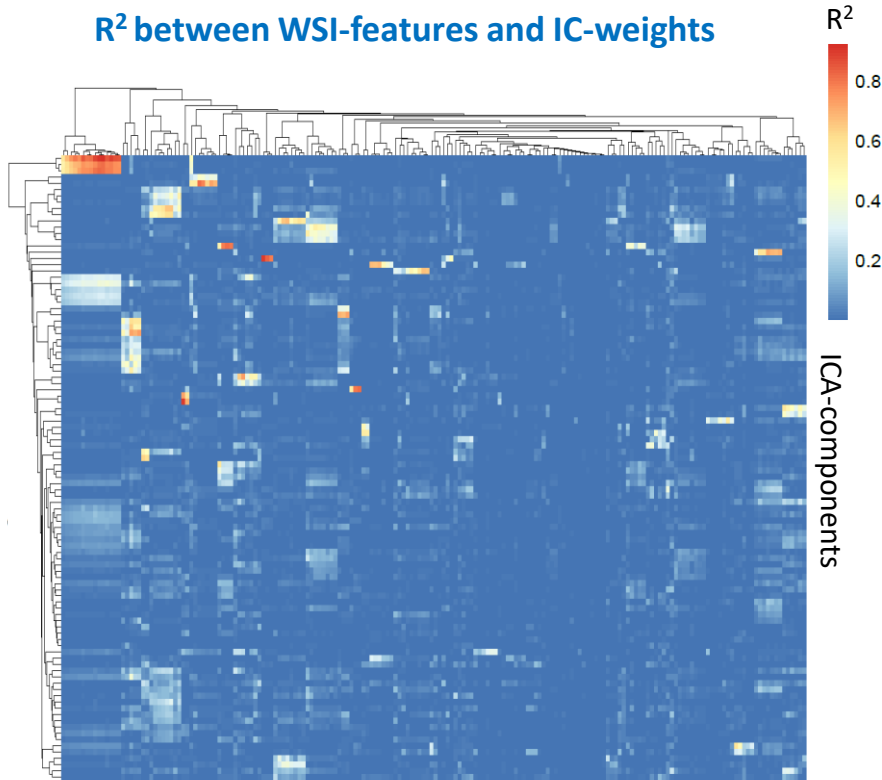
Xception
model: Images

ICA-weights:
RNA-seq

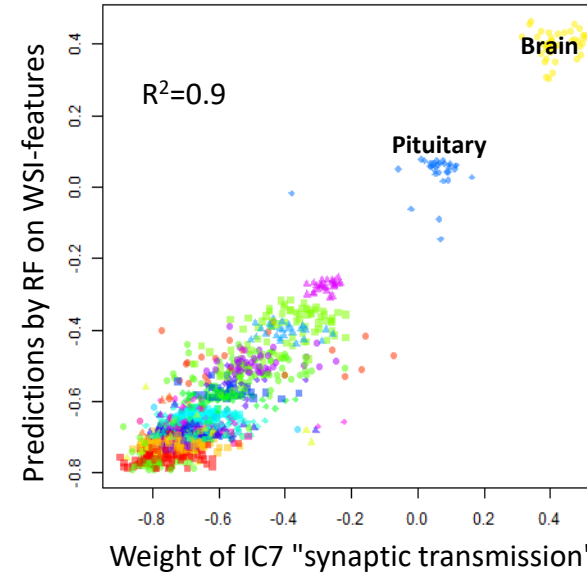
- Adipose Tissue
- Adrenal Gland
- Bladder
- Blood Vessel
- Brain
- Breast
- Colon
- Esophagus
- Heart
- Kidney
- Liver
- Lung
- Muscle
- Nerve
- Ovary
- Pancreas
- Pituitary
- Prostate
- Salivary Gland
- Skin
- Small Intestine
- Spleen
- Stomach
- Testis
- Thyroid
- Uterus
- Vagina



R² between WSI-features and IC-weights



Predicting IC-weight



GO:BP linked to IC7	FDR
chemical synaptic transmission	8e-28
regulation of membrane potential	8e-28
behavior	4e-22
regulation of ion transport	6e-22
synaptic vesicle cycle	3e-20
cognition	7e-20

Predicting ICA-components

- 20% of the components were predicted with $R^2 > 0.9$
- 89% – with $R^2 > 0.5$



A deep learning model to predict RNA-Seq expression of tumours from whole slide images

Benoit Schmauch¹, Alberto Romagnoni^{1,4}, Elodie Pronier^{1,4}, Charlie Saillard¹, Pascale Maille^{2,3}, Julien Calderaro^{2,3}, Aurélie Kamoun¹, Meriem Setta¹, Sylvain Toldo¹, Mikhail Zaslavskiy¹, Thomas Clozel¹, Matali Moarii¹, Pierre Courtiol^{1,5} & Gilles Wainrib^{1,5}

Predicting genes

- 0.4% of the genes showed $R^2 > 0.9$
- 28% – $R^2 > 0.5$

- Deep Learning Networks could be used for feature extraction
- Image features could be used to predict deconvolved signals
- Deconvolved ("clean") signals are better predicted than genes (and related GO gene sets)
- Combining molecular and his histopathological data may:
 - Help pathologists faster and more accurate classify samples
 - Improve accuracy of automatic data analysis
- Spatial transcriptomics, perhaps is our future 😊

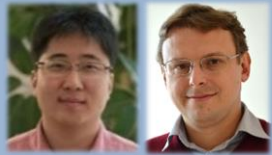
Acknowledgements

Bioinformatics Platform

@ Data Integration and Analysis unit



R. Toth
V. Despotovic
L. Zhang
T. Koma
A. Muller



S.-Y. Kim
P. Nazarov



A. Aalto
Y. Zhang
B. Nosirov
T. Lukashiv



NORLUX @ DoCR



Multomics Data Science
group @ Cancer Research

Key internal collaborators



Simone
Niclou



Anna
Golebiewska



Michel
Mittelbronn



LUXGEN

Interns / students



Maryna
Chepeleva
(PhD student)



Aliaksandra
Kakoichankava
(PhD student)



Yibioa
Wang
(MSc)



Thomas
Eveno
(MSc)



Laurene
Picandet
(MSc)

Key external collaborators



LSRU, Uni Luxembourg
Stephanie Kreis



Institute Curie, France
Andrei Zinovyev



DKFZ, Heidelberg
Jörg Hoheisel
Andrea Bauer
Nathalia Giese



Fonds National de la
Recherche Luxembourg

Supported by FNR Luxembourg. Grants:

- C17/BM/11664971/**DEMICS**
- C21/BM/15739125/**DIOMEDES**